Postprint of: Szymczak C., Kujawa M.: Buckling and initial post-local buckling behaviour of cold-formed channel member flange. THIN-WALLED STRUCTURES. Vol. 137 (2019), pp. 177-184. DOI: 10.1016/j.tws.2019.01.011

Buckling and initial post-local buckling behaviour of cold-formed channel member flange

Czesław Szymczak[1], Marcin Kujawa[2,*]

Gdańsk University of Technology
G. Narutowicza 11/12, 13 80-233 Gdańsk Poland

Abstract

The initial post-buckling behaviour of a cold-formed channel member flange after its local buckling is investigated. An axially compressed column or beam subjected to pure bending is considered. The member material is assumed to follow a linear stress-strain relationship. The governing non-linear differential equation of the problem is derived using the minimum total potential energy principle. An approximate solution for the equation is found by means of the perturbation approach, which allows obtaining the critical buckling stress and the initial post-buckling equilibrium path. The bifurcation point is shown to be symmetric and stable. The proposed analytical solution is compared with finite element method (FEM) and finite strip method (FSM) results to check the validity and range of applicability.

Keywords: Channel cold-formed members, Local buckling, Initial post-buckling behaviour, Closed-form analytical solution, FEM, FSM

1. Introduction

Cold-formed thin-walled channel members are widely applied in various engineering structures. Subjecting the members to bending or compression yields stability problems, global, distortional or local buckling decisive in its design [1], [2]. Some other earlier papers are also worth noting [3], [4], [5], but particularly important are works devoted to methods of buckling and post-buckling analysis [6], [7], [8], [9], [10], [11], [12], [13]. Thus, the member design is carried out in an elastic or a non-linear elastic range of material. Recent developments in theoretical and numerical stability analysis [14], [15] enable the formulation and solution of optimal design of the channel beams [16], [17]. The analytical

*Corresponding author
Email address: mark@pg.edu.pl (Marcin Kujawa)
[1]Faculty of Ocean Engineering and Ship Technology, Department of Structural Engineering
[2]Faculty of Civil and Environmental Engineering, Department of Structural Mechanics

approximate solution for local buckling of compressed beam flanges is very useful in formulation of the optimization problem [18]. The analytical formulae applied in these problems for the critical local buckling stress are derived with approximate assumptions: only the first buckling mode is taken into account and computed without any cooperation of a compressed flange with a beam web.

The main purpose of this investigation is to provide a more accurate analytical description of local buckling and initial post-buckling behaviour of the member compressed flange within an elastic range of material behaviour. A standard channel section is considered. The non-linear differential equation of the stability problem is derived by means of the stationary total energy principle. In the total potential energy formulation, a flange-web cooperation is taken into account. The perturbation approach applied to solve the equation leads to the buckling stresses related to the number of half-wave modes and the initial post-buckling equilibrium path. The critical buckling stress and corresponding mode are found at the minimum value of the buckling stresses obtained. Moreover, the relation of the critical stress and the relative member length derived makes it possible to find the number of half-waves of the buckling mode. The initial post-buckling equilibrium paths allow classifying all bifurcation points as symmetric and stable. Some numerical examples dealing with simply supported beams and columns are presented here.

This paper continues our research related to buckling of thin-walled columns in the non-linear range [19], [20], [21].

2. Total potential energy of member flange

Let us consider a channel beam undergoing pure bending or an axially compressed channel column as shown in Fig. 1. Local buckling of the compressed member flange and its initial post-buckling behaviour are investigated. It is assumed that the member material follows Hooke's law. The Cartesian coordinate system x, y, z is located at the centre of flange rotation. If the flange rotates about the line of connection with the web, then the displacements $v(z)$ of arbitrary points $x(z)$ of the flange may be written as (see Fig. 1)

$$v = x \sin\theta \tag{1}$$

where the angle of cross-sectional rotation is denoted by θ. The flange-web cooperation is represented by springs uniformly distributed along the connection line. The elastic moduli of the springs k_θ are different for the beam and the column and may be written as

$$k_\theta = \chi \frac{EI_w}{h} \tag{2}$$

where EI_w denotes the bending stiffness of the web, h is the web height and we assume the coefficients χ=4 for beams and χ=2 for columns [22] (see Appendix A).

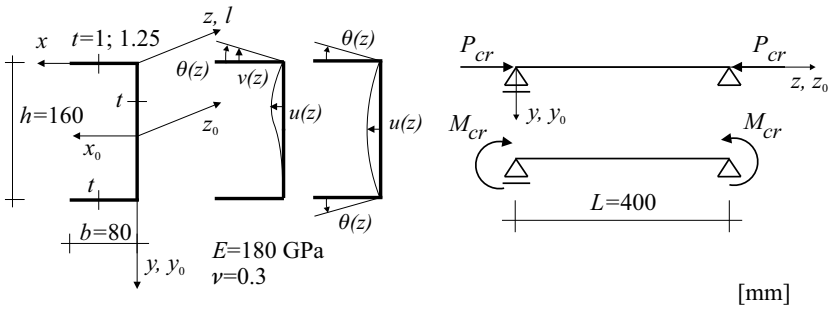

Figure 1: Displacements of members's flanges and data of numerical examples

The total potential energy of the flange V in the initial post-buckling state consists of the elastic strain energy of the flange V_e, the potential energy of the springs V_s and the potential energy V_l of the uniformly distributed normal stresses σ_0 applied in the flange cross-section

$$V = V_e + V_s + V_l. \tag{3}$$

The elastic strain energy in the initial post-buckling state is the sum of the effects of bending and free torsion of the flange and may [23] be expressed as follows:

$$V_e = \frac{1}{2}E\int_0^l\int_0^b i_x v''^2 dA dz + \frac{1}{2}GI_d\int_0^l \theta'^2 dz + \frac{1}{8}E\overline{I}_{00}\int_0^l \theta'^4 dz \tag{4}$$

where E is Young's modulus, G is the shear modulus, I_d stands for the free torsion moment of inertia of the flange cross-section and i_x denotes the second moment of inertia of a unit flange length about the x axis. Moreover, by $\overline{I}_{00} = I_{00} - \frac{{I_0}^2}{A}$, the reduced fourth-order polar moment of the flange cross-section is denoted. Here, I_0 is the polar moment of inertia, I_{00} is the fourth-order polar moment of inertia, $A = bt$ stands for the flange cross-section and l stands for the member length.
Applying the relation (1) and expanding the functions $\sin\theta$ into the Taylor's series after some algebra, Eq. (4) may be rewritten as

$$V_e = \frac{1}{2}E\int_0^l \Big[\overline{I}_x\Big(\theta''^2 - 2\theta\theta'^2\theta'' - \theta^2\theta''^2\Big) + \frac{GI_d\theta'^2}{E} + \frac{1}{4}\overline{I}_{00}\theta'^4\Big]dz \tag{5}$$

where $\overline{I}_x = \int_0^b I_x(x)x^2dx$ defines the fourth-order inertia moment of the flange. The powers of the rotation angle and its derivatives higher than the fourth are omitted.

The potential energy of the applied normal stresses σ_0 due to the flange rotation is

$$V_l = -\frac{1}{2}\sigma_0\int_0^l\int_A v'^2 dA dz. \tag{6}$$

Similarly, the relations (1) are applied in equation (6); thus, we arrive at

$$V_l = -\frac{1}{2}\sigma_0 I_y \int_0^l \Big(\theta'^2 - \theta'^2\theta^2\Big)dz \tag{7}$$

where I_y denotes the second-order moment of inertia of the flange cross-section about axis y located in the rotation centre of the flange (see Fig. (1)).

The last part of the total potential energy accounting for the uniformly distributed springs may be written as

$$V_s = \frac{1}{2}k_\theta \int_0^l \theta^2 dz \tag{8}$$

where k_θ is defined in (2).

Summing up all parts of the total potential energy (5), (7) and (8), the final formulae can be presented as a functional

$$V = \frac{1}{2}\int_0^l F(\theta, \theta', \theta'')dz \tag{9}$$

where the under-integral function is defined as

$$\begin{aligned} F(\theta,\theta',\theta'') &= E\Big[\overline{I}_x\Big(\theta''^2 - \theta''^2\theta^2 - 2\theta\theta'^2\theta'' + \frac{1}{4}\overline{I}_{00}\theta'^4\Big)\Big] + ... \\ &+ GI_d\theta'^2 + k_\theta\theta^2 - \sigma_0 I_y\theta'^2\Big(1-\theta^2\Big). \end{aligned} \tag{10}$$

3. Local buckling and initial post-buckling behaviour

The non-linear differential equation of equilibrium of the flange resulting from the Euler condition of stationary total potential energy (9) [24] can be written as

$$\begin{aligned} \theta^{IV} + 2\alpha\theta'' + \beta^2\theta &= \theta^{IV}\theta^2 + 6\theta'^2\theta'' + 4\theta\theta'\theta''' + 3\theta\theta''^2 + ... \\ &+ \frac{3\overline{I}_{00}}{2\overline{I}_x}\theta'^2\theta'' + \frac{\sigma_0 I_y}{E\overline{I}_x}\Big(\theta''\theta^2 + \theta\theta'^2 - \theta''\Big) \end{aligned} \tag{11}$$

where

$$\begin{aligned} 2\alpha &= \frac{\sigma_0 I_y - GI_d}{E\overline{I}_x} \\ \beta^2 &= \frac{k_\theta}{E\overline{I}_x}. \end{aligned} \tag{12}$$

Applying the perturbation approach, the solution of Eq. (11) is determined [23], [25]. The flange angle of rotation can be represented as a polynomial of the perturbation parameter s

$$\theta(s) = s\theta_1(s) + s^2\theta_2(s) + s^3\theta_3(s) + ... \tag{13}$$

where $\theta_i(z)$ for i=1, 2, 3 stand for functions of z that should fulfil suitable boundary conditions.

The stress σ_0 can be also expressed in the same form

$$\sigma_0 = \sigma_{cr} + \sigma^{(1)} s + \sigma^{(2)} s^2 + ... \tag{14}$$

where σ_{cr} stands for the critical buckling stress and by $\sigma^{(i)}$ the i-th derivative of the stress σ with respect to s is denoted.

Moreover, it is assumed that the perturbation parameter is equal to the maximum angle of rotation $s = \theta_0 = \theta(z_0)$ located at z_0; hence, using the relation (13), some additional boundary conditions are established

$$\theta_1(z_0) = 1, \quad \theta_i(z_0) = 0 \quad \text{for} \quad i \neq 1. \tag{15}$$

Applying the relations (13) and (14) in the non-linear differential equation (11) and coefficients of the first power of s equal to zero, the following linear differential equation reads

$$\theta_1^{IV} + 2\alpha\theta_1'' + \beta^2\theta_1 = 0. \tag{16}$$

The solution of Eq. (16) can be written as

$$\theta_1 = C_1 \sin k_1 z + C_2 \cos k_1 z + C_3 \sin k_2 z + C_4 \cos k_2 z \tag{17}$$

where

$$k_1 = \sqrt{\alpha\Big(1 - \sqrt{1 - \big(\beta/\alpha\big)^2}\Big)}, \quad k_2 = \sqrt{\alpha\Big(1 + \sqrt{1 - \big(\beta/\alpha\big)^2}\Big)}. \tag{18}$$

The constants C_1, C_2, C_3 and C_4 should be determined from suitable boundary conditions. Let us consider a simply supported member as shown in Fig. 1. The boundary conditions defined as follows:

$$\theta_1(z=0) = \theta_1''(z=0) = 0, \quad \theta_1(z=l) = \theta_1''(z=l) = 0 \tag{19}$$

together with the additional condition (15) enables obtaining the buckling stress

$$\sigma_b = \frac{E}{I_y}\Big(\overline{I}_x m^2 + \frac{\chi I_w}{h m^2} + \frac{G I_d}{E}\Big) \tag{20}$$

and the buckling mode

$$\theta_1 = \sin mz \tag{21}$$

where $m = \frac{n\pi}{L}$ and n stands for number of the half-waves of the buckling mode. The number n should be chosen to obtain the minimum critical stress. Hence, it is possible to determine the location of the maximum angle of torsion $z_0 = \frac{L}{2n}$ (15) in the middle of the half-wave.

It is useful to know a relation between the critical stress and the member length that makes possible finding the number of the half-waves n. As mentioned above, the critical stress should be determined to obtain the minimum buckling stress. The necessary condition for the minimum buckling stress with respect to m is

$$\frac{d\sigma_b}{dm} = 2m\overline{I}_x - \frac{2\chi I_w}{hm^3} = 0. \tag{22}$$

Hence,

$$m = \sqrt[4]{\frac{\chi I_w}{h\overline{I}_x}}. \tag{23}$$

The equation (23) makes possible determining the member length corresponding to the stress minimum

$$L = n\pi\sqrt[4]{\frac{h\overline{I}_x}{\chi I_w}}. \tag{24}$$

Following [26], it is useful to introduce a characteristic length L_0

$$L_0 = \pi\sqrt[4]{\frac{h\overline{I}_x}{\chi I_w}}. \tag{25}$$

Substitution of Eq. (24) into Eq. (20) leads to the minimum value of the stress that occurs in each member with a length $L = \eta L_0$

$$\sigma_{min} = \frac{E}{I_y}\Big(2\sqrt{\frac{\chi I_w \overline{I}_x}{h}} + \frac{GI_d}{E}\Big). \tag{26}$$

The relation of the critical buckling stress and a scaling coefficient $\eta = \frac{L}{L_0}$ is shown in Fig. 2, where not only critical stress but also a number n of half-waves of the buckling mode can be found.

The coefficient of the second power of s leads to the next differential equation

$$\theta_2^{IV} + 2\alpha\theta_2'' + \beta^2\theta_2 = -\frac{\sigma^{(1)}\theta_1'' I_y}{E\overline{I}_x}. \tag{27}$$

Making use of the buckling mode (21) in (27) and noticing that left side of this equation is the same as the previous equation (16), it is easy to find

$$\theta_2 = 0 \quad \text{and} \quad \sigma^{(1)} = 0. \tag{28}$$

This equation means that the bifurcation point is symmetrical [25].
The third term of the power series in s leads to the third linear differential equation

$$\begin{aligned}\theta_3^{IV} + 2\alpha\theta_3'' + \beta^2\theta_3 &= \theta_1^{IV}\theta_1^2 + 6{\theta_1'}^2\theta_1'' + 4\theta_1\theta_1'\theta_1''' + 3\theta_1{\theta_1''}^2 + ... \\ &- \frac{\sigma^{(2)}\theta_1'' I_y}{E\overline{I}_x} + \frac{3\overline{I}_{00}}{2\overline{I}_x}{\theta_1'}^2\theta_1'' + \frac{\sigma_{cr} I_y}{E\overline{I}_x}\Big(\theta''\theta^2 + \theta{\theta'}^2\Big).\end{aligned} \tag{29}$$

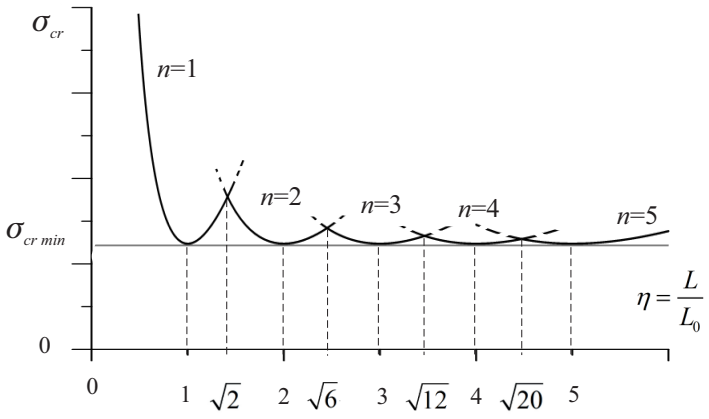

Figure 2: Critical buckling stress vs. scaling coefficient η

Substituting the buckling mode (21) into Eq. (29) and applying trigonometric relations, Eq. (29) can be rewritten as

$$\theta_3^{IV} + 2\alpha\theta_3'' + \beta^2\theta_3 = k_3 \sin mz + l_3 \sin 3mz \tag{30}$$

where

$$\begin{aligned} k_3 &= \frac{m^2}{8E\overline{I}_x}\Big[E\big(4\overline{I}_x - 3\overline{I}_{00}\big)m^2 + I_y\big(8\sigma^{(2)} - 4\sigma_{cr}\big)\Big] \\ l_3 &= \frac{m^2}{8E\overline{I}_x}\Big[4I_y\sigma_{cr} - E\big(3\overline{I}_{00} + 28\overline{I}_x\big)m^2\Big]. \end{aligned} \tag{31}$$

The solution of equation (30) is

$$\begin{aligned} \theta_3 = C_1 \sin k_1 z + C_2 \cos k_1 z &+ C_3 \sin k_2 z + C_4 \cos k_2 z + ... \\ &+ K_3 \sin mz + L_3 \sin 3mz \end{aligned} \tag{32}$$

where

$$\begin{aligned} K_3 &= \frac{k_3}{m^4 - 2\alpha m^2 + \beta^2} \\ L_3 &= \frac{l_3}{81m^4 - 18\alpha m^2 + \beta^2}. \end{aligned} \tag{33}$$

The constants C_1, C_2, C_3 and C_4 should be computed by applying boundary conditions (23) and the additional condition (15). Thus, we arrive at

$$\theta_3 = L_3\big(\sin mz + \sin 3mz\big) \quad \text{and} \quad K_3 = 0. \tag{34}$$

The first relation (32) incorporated into Eq. (14) and after substitution of the buckling mode (21) leads to the initial post-buckling shape of the torsional angle

$$\theta = \theta_0 \sin mz + \theta_0^3 L_3\big(\sin mz + \sin 3mz\big). \tag{35}$$

The first equation (31) allows to obtain $\sigma^{(2)}$ (see Eq. (14)) determining the initial curvature of the post-buckling equilibrium path

$$\sigma^{(2)} = \frac{GI_d}{2I_y}\Big[1 + \frac{E\big(3h\bar{I}_{00}m^4 + 4I_w\chi\big)}{4GhI_dm^2}\Big]. \tag{36}$$

Finally, the initial post-buckling equilibrium path may be written in an approximate form as

$$\frac{\sigma}{\sigma_{cr}} = 1 + \frac{\sigma^{(2)}}{\sigma_{cr}}\theta^2. \tag{37}$$

The positive value of $\sigma^{(2)}$ (see (36)) together with $\sigma^{(1)} = 0$ (see (28)) shows that the symmetrical stable bifurcation point always exists, given any geometrical and mechanical parameters; i.e., no critical stress reduction is possible due to the inevitable initial angle of flange rotation.

4. Numerical examples

Let us consider an example of a simply supported beam undergoing pure bending and an axially compressed column made of nickel alloy [27] (E=180 GPa, v=0.3, ρ=8500 kg/m^3, σ_{pl}=900 MPa) as shown in Figs. 1 and 3. Two thickness variants t=1 and t=1.25 mm of cross-sections are investigated. The analytical solutions are compared with the numerical ones. Numerical analysis is conducted using FEM (ABAQUS) [28] and additional FSM (CUFSM) [29]. To estimate the values of critical buckling loads and post-buckling equilibrium paths, linear perturbation (LBA) and dynamic implicit quasi-static procedures are used [30]. In the case of axially compressed columns, it is assumed that the load increases in a single step up to 100 N, and in the case of pure bending, the moment is not greater than 10 Nm. In the FEM analysis, the members are modelled by means of shell elements with reduced integration type S4R; i.e., 80 elements are along the cross-section and 100 elements along the length of the member. In Fig. 3, numerical models, load and imposed boundary conditions are shown. The FEM calculations were performed with the use of two models: the first *Model A* to find a starting non-perfect geometry using kinematic extortion for column and beam (see Fig. 3a) and the second *Model B* used in the main analysis without or with initial imperfections (see Fig. 3b). The critical buckling stresses and corresponding number of half-waves are determined for all cases and shown in Tab. 1. The graphical presentation of the post-critical stress vs. torsional angle amplitude is shown for columns in Fig. 4 and for beams in Fig. 5.

Additionally, the characteristic member lengths and the minimum critical buckling stresses for all cases of members and both thicknesses under investigation are determined and presented in Tab. 2. In this table, the relative curvatures of the initial post-buckling paths (37) and the coefficients L_3 (33) determining the initial post-buckling behaviour of the flange rotation angle are also presented.

Table 1: Critical local buckling stress of axially compressed columns and beams undergoing pure bending

t [mm]	Number of half-waves n				σ_{cr} [MPa]			
	Analyt.	FEM		FSM	Analyt.	FEM		FSM
		LBA	Quasi static			LBA	Quasi static	
Axially compressed column								
1	(η=2.1) 2	2	2	2	18.97	18.42	18.74	18.55
1.25	(η=2.1) 2	2	2	2	29.64	28.75	28.99	28.98
Beam undergoing pure bending								
1	(η=2.5) 3	2	2	2	23.10	23.48	24.00	23.41
1.25	(η=2.5) 3	2	2	2	36.10	36.63	37.01	36.57

The geometrical characteristic of channel cross-sections necessary to calculate the stresses and the initial post-buckling path are as follows

$$I_d = \frac{t^3 b}{3}, \quad I_y = \frac{t b^3}{3}, \quad \overline{I}_x = \frac{b^3 t^3}{36}, \quad \overline{I}_{00} = \frac{t b^5}{180}, \quad I_w = \frac{t^3}{12}. \tag{38}$$

The characteristic member length (25) may be determined directly by the dimensions of the cross-section as

$$L_0 = \pi b \sqrt[4]{\frac{h}{3\chi b}}. \tag{39}$$

Similarly the buckling stress (20), minimum buckling stress (26) and $\sigma^{(2)}$ (36) may be presented in the forms

$$\sigma_b = \frac{t^3 E m^2}{12}\Big[1 + \frac{3\big(4bGhm^2 + E\chi\big)}{b^3 E h m^4}\Big], \tag{40}$$

$$\sigma_{min} = E\Big(\frac{t}{b}\Big)^2\Big(\frac{1}{2}\sqrt{\frac{\chi b}{3h}} + \frac{G}{E}\Big), \tag{41}$$

$$\sigma^{(2)} = \frac{G t^2}{2b^2}\Big[1 + \frac{E\big(b^5 h m^4 + 20 t^2 \chi\big)}{80 bGh m^2 t^2}\Big]. \tag{42}$$

The positive value of Eq. (42) points out that the initial curvatures of the post-buckling equilibrium path are always positive. This observation together with (25) determines the symmetrical and stable points of bifurcations [23], [25], in which decreases in the buckling stresses are not possible. The critical stresses of beams undergoing pure bending are higher than the same stresses

Table 2: Characteristic column and beam lengths, minimum critical stresses, $\sigma^{(2)}/\sigma_{cr}$ and L_3

t [mm]	σ_{min} [MPa]	L_0 [mm]	$\sigma^{(2)}/\sigma_{cr}$ [-]	L_3
Axially compressed column				
1	18.94	190.97	94.1	-7.7
1.25	29.59	190.97	60.3	-4.9
Beam undergoing pure bending				
1	22.30	160.58	173.3	-7.1
1.25	34.84	160.58	111.1	-4.5

of axially compressed columns due to more effective flange-web cooperation. It may be concluded that the critical stresses increase with the element stiffness. The number of the mode half-waves depends on the cross-sectional geometry, and the values in beams are usually higher or equal to those in columns (see Tab. 1).
The buckling modes and initial post-buckling distribution of the flange angle along the columns axes are presented in Fig. 6 along the beam axes in Fig. 7. The amplitude of the buckling mode is assumed to be 0.01 rad.

5. Conclusions

The focus of this paper is local buckling of the compressed flanges of cold-formed channel beams undergoing pure bending and axially compressed columns. The total potential energy formulation allows derivation of the non-linear differential equation governing the buckling and the initial post-buckling behaviour of the flanges. A simple model of the flange is assumed in the form of a beam rigid in its plane and elastically connected with the member web. The solution for the equation is determined by means of the perturbation approach. The critical buckling stress and corresponding number of half-waves are determined. Moreover, the characteristic member length is introduced, making it possible to directly assess the number of half-waves related to the member length.

The theoretical and numerical investigations of the local buckling and initial post-buckling behaviour of the member flanges lead to drawing the following conclusions related to the investigated problems:

- The points of bifurcation of local flange buckling are symmetrical and stable in all considered cases. The term $\sigma^{(2)}$ (35) denoting the curvature of the initial post buckling path is positive for beams and columns. This result means that no decrement occurs in the critical stresses due to inevitable geometrical imperfections of the flange torsional angle.
- The critical stresses of the beam flanges are higher than the column case values due to more effective flange-web cooperation. A greater flange thickness leads to higher critical buckling stresses.

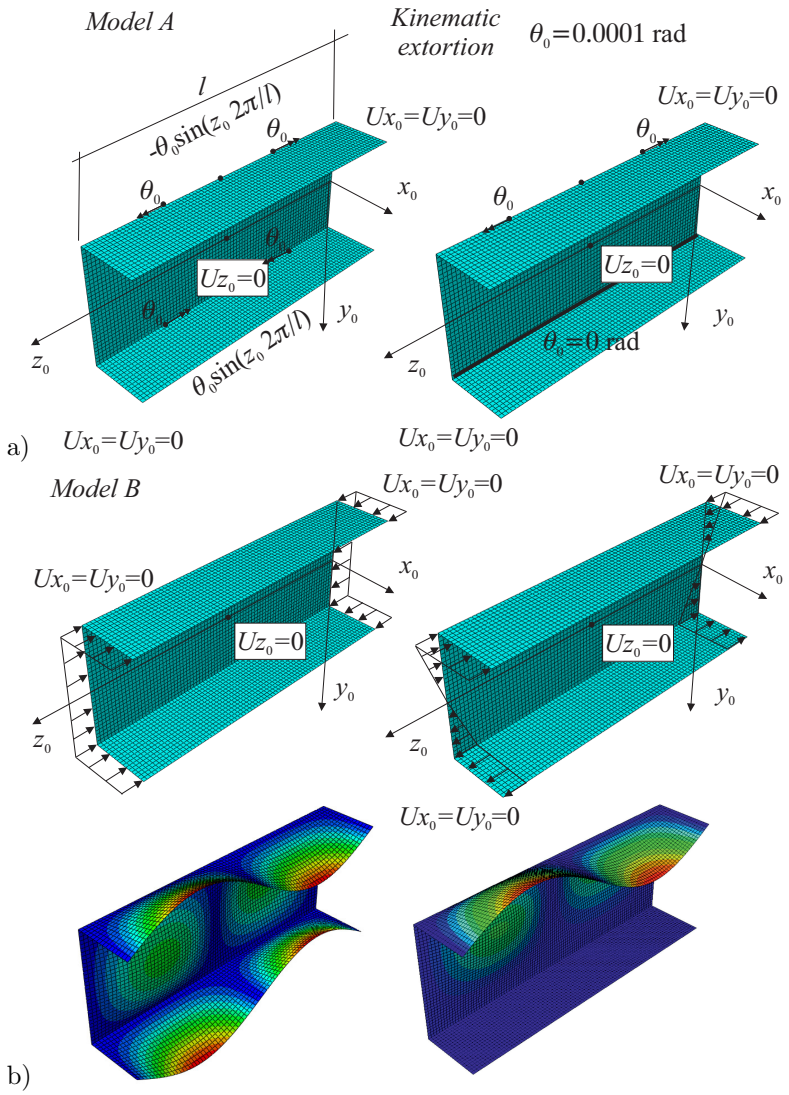

Figure 3: Finite element models, boundary conditions for model with or without initial imperfections, load diagrams and exemplary buckling modes for axially compressed columns or beams undergoing pure bending at number of half-waves n=2

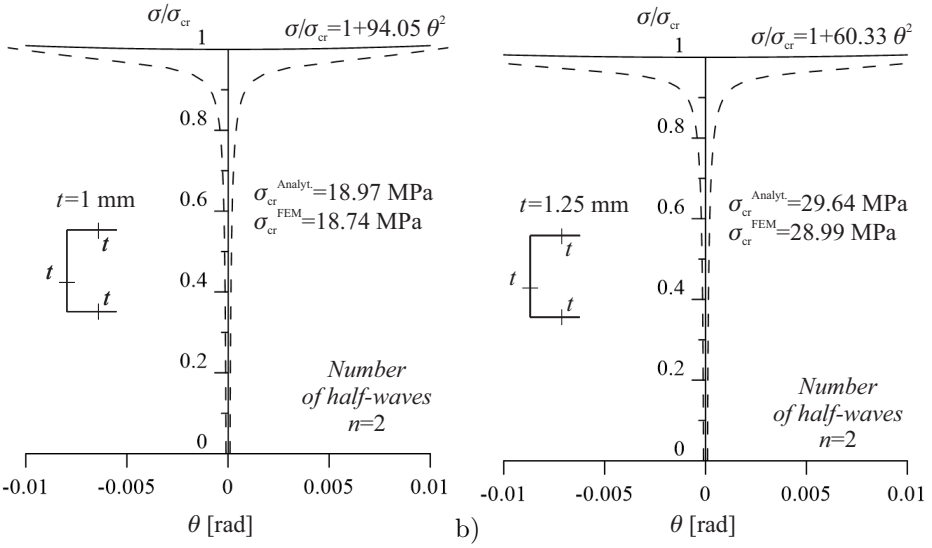

Figure 4: Post-critical stresses vs. torsion angle amplitude for simply supported columns for a) t=1 mm and b) t=1.25 mm

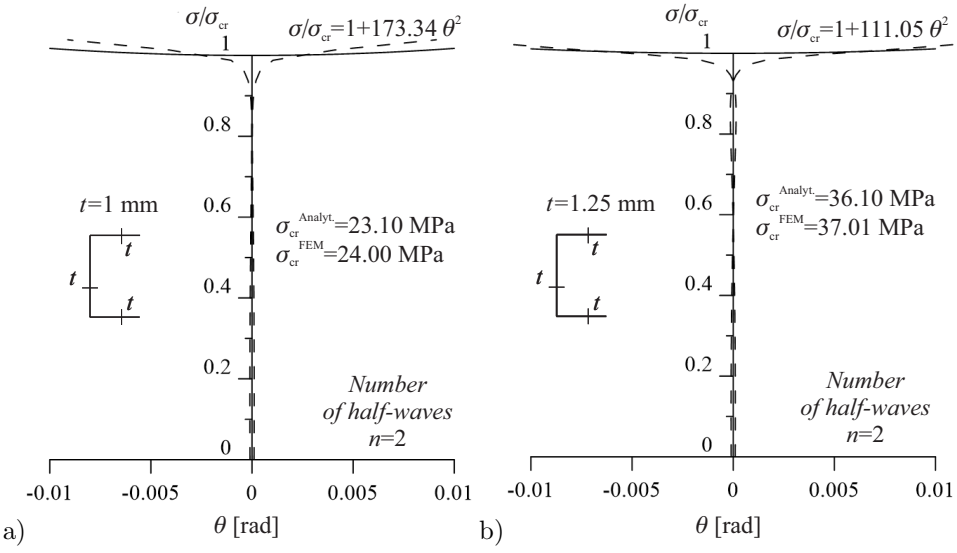

Figure 5: Post-critical stresses vs. torsion angle amplitude for simply supported beams for a) t=1 mm and b) t=1.25 mm

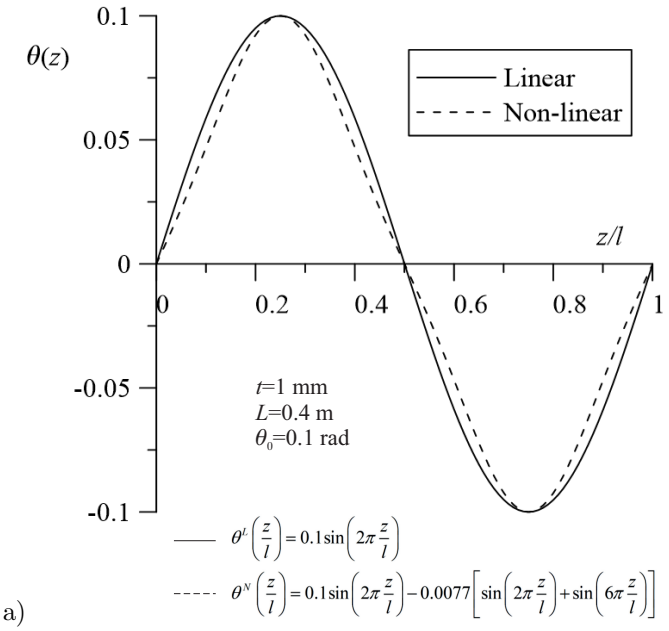

a)

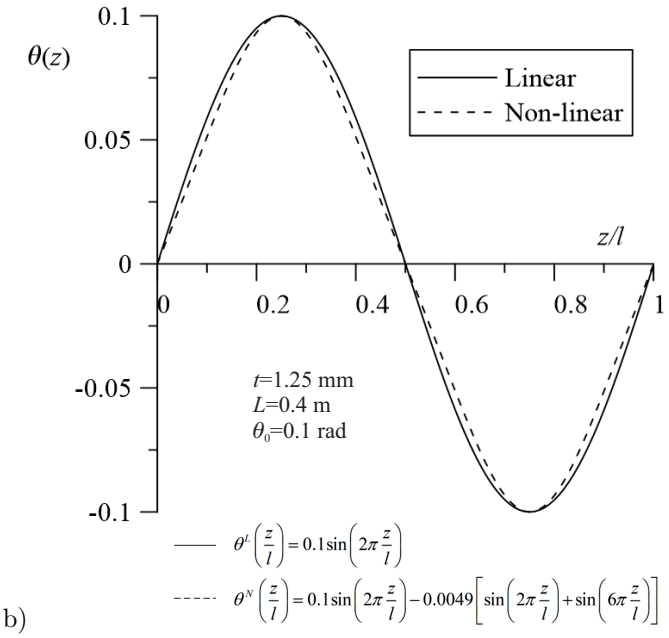

b)

Figure 6: Buckling mode and post-buckling shape of the flange angle of rotation vs. its amplitude for columns with a) t=1 mm and b) t=1.25 mm

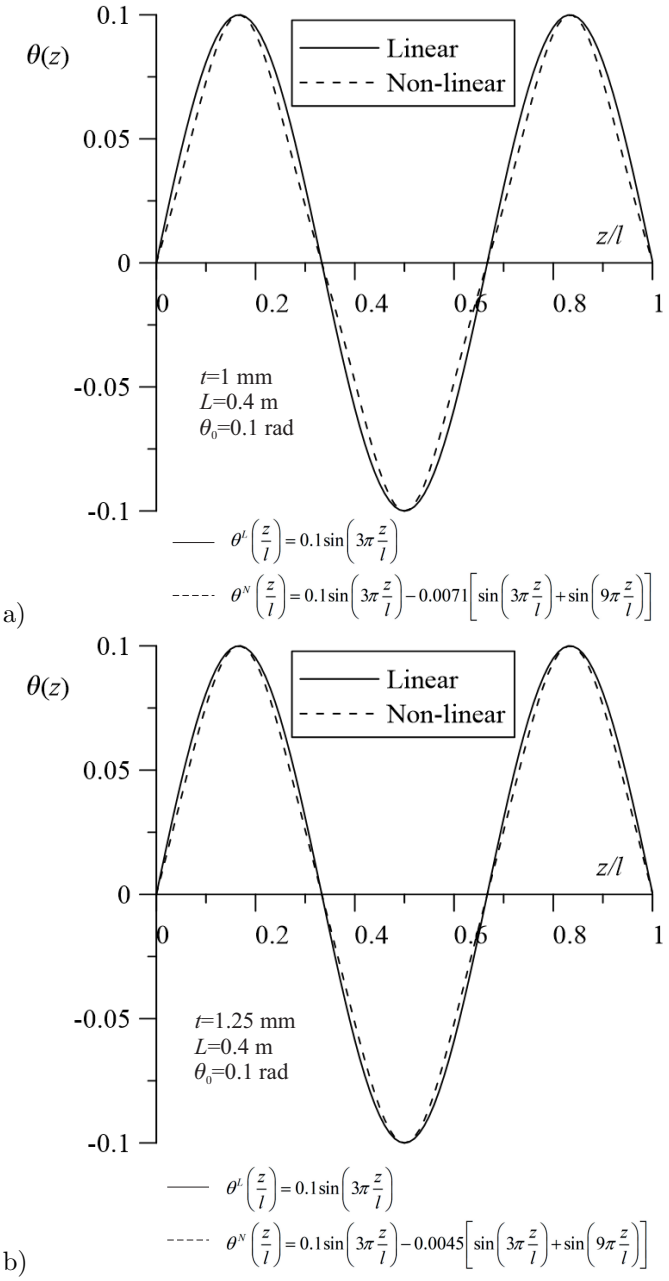

Figure 7: Buckling mode and post-buckling shape of the flange angle of rotation vs. its amplitude for beams with a) t=1 mm and b) t=1.25 mm

- The number of mode half-waves depends on the flange bending stiffness and is different for beams and columns with respect to the effect of the flange-web cooperation. A greater flange stiffness triggers a lower number of half-waves. The number of beam half-waves is usually higher than or equal to the value in the column case. It should be noted that in many approximate solutions of similar problems [31], [32], only the first mode is taken into account and that no flange-web cooperation is considered. Such assumptions may lead to qualitative and numerical errors. The derived analytical formulas for critical buckling stress may be useful in preliminary design and optimization of this type of structure.

References

[1] J. Davies, Recent advances in cold-formed steel structures, Journal of Constructional Steel Research 55 (2000) 267–288.

[2] G. Hancock, Cold-formed steel structures, Journal of Constructional Research 59 (2003) 473–487.

[3] G. Hancock, Distortional buckling of steel storage rack columns, Journal of Structural Engineering ASCE 111 (1985) 2770–2783.

[4] S. Lau, G. Hancock, Distortional buckling formulas for channel columns, Journal of Structural Engineering ASCE 113 (1987) 1063–1078.

[5] Y. Kwon, G. Hancock, Strength test of cold-formed channel sections undergoing local and distortional buckling, Journal of Structural Engineering ASCE 117 (1992) 1786–1803.

[6] Y. Cheung, Finite strip method in structural analysis, Pergamon Press, 1976.

[7] Y. Kwon, G. Hancock, A nonlinear elastic spline finite strip analysis for thin-walled sections, Thin-Walled Structures 12 (1991) 295–319.

[8] Y. Cheung, L. Tham, Finite strip method, CRC Press, 1998.

[9] R. Schardt, Generalized beam theory - an adequate method for stability problems, Thin-Walled Structures 19 (1994) 161–180.

[10] D. Camotim, C. Basaglia, N. Silvestre, GTB buckling analysis of thin-walled steel frames: A state-of-the-art report, Thin-Walled Structures 48 (2010) 726–743.

[11] J. Teng, J. Zhao, Distortional buckling of channel beam-columns, Thin-Walled Structures 41 (2003) 595–617.

[12] A. van der Heijden (Ed.), W.T. Koiter's elastic stbility of solids and structures, Cambridge University Press, 2009.

[13] Z. Li, J. Abreu, J. Leng, B. Schafer, Review: Constrined finite strip method developmnents and application in cold-formed steel design, Thin-Walled Structures 81 (2014) 2–18.

[14] M. Mcdonald, M. Heiyantuduwa, J. Rhodes, Recent developments in design of cold-formed steel members and structures, Thin-Walled Structures 46 (2008) 1047–1053.

[15] K. Magnucki, W. Szyc, P. Stasiewicz, Stress state and elastic buckling of a thin-walled beam with monosymmetric open cross-section, Thin-Walled Structures 42 (2008) 25–38.

[16] E. Magnucka-Blandzi, K. Magnucki, Buckling and optimal design of cold-formed beams; reviews of selected problem, Thin-Walled Structures 46 (2011) 554–561.

[17] K. Magnucki, M. Ostwald, Optimal design of selected open-cross-sections of cold-formed thin-walled beams, Publishing House of Poznan University of Technology, 2005.

[18] K. Magnucki, P. Paczos, Theoretical shape optimization of cold-formed thin-walled channel beams with drop flanges in pure bending, Journal of Constructional Steel Research 65 (2009) 1731–1737.

[19] C. Szymczak, M. Kujawa, Torsional buckling and post-buckling of columns made of aluminium alloys, Applied Mathematical Modelling 60 (2018) 711–720.

[20] C. Szymczak, M. Kujawa, Buckling of thin-walled columns accounting for initial geometrical imperfections, International Journal of Non-Linear Mechanics 95 (2017) 1–9.

[21] C. Szymczak, M. Kujawa, Flexural buckling and post-buckling of columns made of aluminium alloy, European Journal of Mechanics A/Solids 73 (2019) 420–429.

[22] S. Timoshenko, D. Young, Theory of structures, McGraw-Hill, 1965.

[23] C. Szymczak, Buckling and initial post-buckling behavior of thin-walled I columns, Computers and Structures 11 (1980) 481–487.

[24] I. Gelfand, S. Fomin, Calculus of variations, Prentice-Hall, Inc., Englewood Cliffs, 1963.

[25] J. Thompson, G. Hunt, A general theory of elastic stability, John Wiley and Sons, 1973.

[26] C. Szymczak, M. Kujawa, On local buckling of cold-formed channel members, Thin-Walled Structures 106 (2016) 93–101.

[27] J. Everhart, Engineering properties of nickel and nickel alloys, Plenum Press, 1971.

[28] D. Habbit, B. Karlsson, P. Sorensen, ABAQUS analysis user's manual, Hibbit, Karlsson, Sorensen Inc.

[29] Z. Li, B. Schafer. CUFSM elastic buckling analysis of thin-walled members with general end boundary conditions [online, cited http://www.ce.jhu.edu/bschafer/cufsm/].

[30] M. Kujawa, Selected local stability problems of channel section flanges made of aluminium alloys, Continuum Mechanics and Thermodynamics (2018) https://doi.org/10.1007/s00161–018–0705–z.

[31] K. Magnucki, P. Paczos, K. Kasprzak, Elastic buckling of cold formed thin-walled channel beams with drop flanges, Journal of Structural Mechanics ASCE 136 (2010) 886–896.

[32] P. Paczos, Experimental investigation of C-beams with non-standard flanges, Journal of Constructional Steel Research 93 (2014) 77–87.

Appendix A. Derivation of χ coefficients

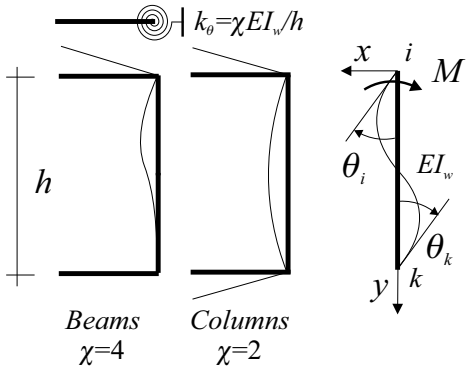

Deflection line

$$
\begin{aligned}
x^{IV} &= p = 0 \\
x'' &= C_1 y + C_2 \\
x' &= C_1 \frac{y^2}{2} + C_2 y + C_3 \\
x &= C_1 \frac{y^3}{6} + C_2 \frac{y^2}{2} + C_3 y + C_4
\end{aligned}
$$

General boundary conditions

$$
\begin{aligned}
y = 0, \quad x = 0, \quad x' = \theta_i \\
y = h, \quad x = 0, \quad x' = \theta_k
\end{aligned}
$$

Integration constants

$$
\left\{
\begin{array}{rcl}
C_4 & = & 0 \\
C_3 & = & \theta_i \\
C_1 \frac{h^3}{6} + C_2 \frac{h^2}{2} + C_3 h + C_4 & = & 0 \\
C_1 \frac{h^2}{2} + C_2 h + C_3 & = & \theta_k
\end{array}
\right.
\Rightarrow
\begin{array}{rcl}
C_1 & = & \frac{6}{h^2}\Big(\theta_i + \theta_k\Big) \\
C_2 & = & -\frac{2}{h}\Big(2\theta_i + \theta_k\Big)
\end{array}
$$

Spring stiffness - general solution

$$
k_\theta = M = -EI_w x''(0) = -EI_w C_2 = \frac{2EI_w}{h}\Big(2\theta_i + \theta_k\Big)
$$

Spring stiffness - beam ($\theta_i = 1$)

$$
k_\theta = M = \frac{2EI_w}{h} 2\theta_i = \frac{4EI_w}{h} = \frac{\chi EI_w}{h} \Rightarrow \chi = 4
$$

Spring stiffness - column ($\theta_i = 1$)

$$
k_\theta = M = \frac{2EI_w}{h}\Big(2\theta_i + \theta_k\Big) = \wr\, \theta_k = -\theta_i \,\wr = \frac{2EI_w}{h} = \frac{\chi EI_w}{h} \Rightarrow \chi = 2
$$